

Integration of radioactive, conventional logs and geochemical analyses to evaluate the hydrocarbon system of Rudeis Formation, October oil field, Gulf of Suez, Egypt

Marwa Z. EL-SAWY¹ , Ibrahim M. AL-ALFY^{2,*} , Sherif FAROUK¹ ,
Tarek F. SHAZLY¹ , Nouran S. SALAMA³ 

¹ Exploration department, Egyptian Petroleum Research Institute (EPRI), Egypt

² Exploration Division, Nuclear Materials Authority, Egypt

³ Geology Department, Faculty of Science, Helwan University, Egypt

Abstract: The objective of this research is to determine the source rock by using a combination of well logging data, spectral gamma-ray logs, as well as laboratory geochemical analysis. This involves quantifying the total organic carbon content (TOC) as a key parameter to study the source rock of Rudeis Formation rocks in the October oil field, Gulf of Suez, Egypt. After theoretical calculations of well logging, the mean TOC value comes out to 1.2 wt%. The TOC values in the lab ranged from 0.4 wt% to 1.4 wt%, with a mean value of 0.9 wt%. According to Rudeis Formation's petrophysical properties, the hydrocarbon saturation levels in the upper and lower Rudeis reservoirs were recorded 57% to 60%, and the percentages of shale content in each reached 63% and 51%, respectively. The Radiogenic Heat Production (RHP) values ranged from $0.85 \mu\text{W}/\text{m}^3$ (minimum) to $2.38 \mu\text{W}/\text{m}^3$ (maximum) with a mean of $1.37 \mu\text{W}/\text{m}^3$ and a standard deviation of approximately $0.19 \mu\text{W}/\text{m}^3$. Five sections along the Rudeis Formation (Source 1 to Source 5) are considered hydrocarbon-bearing zones. Three of the zones were classified as source rocks (Source 2, Source 3, and Source 5) associated with a high volume of shales (mostly clay), while the other two zones (Source 1 and Source 4) are associated with a moderate volume of shales (shaly sandstones) considered to be source and reservoir rocks in the Upper and Lower Rudeis Formation. The lower Rudeis unit appears to have fair to good hydrocarbon potential, with TOC ranging from 0.46 to 1.28 weight percent and S₂ varying from 0.88 to 3.76 mg/g. The upper Rudeis member is classified as a fair oil source rock, based on TOC values ranging from 0.42 to 1.29%. The equations (1), (2) and (3) were found to be the best fit to the TOC data.

Key words: radiogenic heat production, October oil field, total organic carbon, hydrocarbon system

*corresponding author, e-mail: ibelalfy@yahoo.com

1. Introduction

The Gulf of Suez is a Cenozoic extensional rift basin that occupies the northern end of the Red Sea rift; it is one of the world's most prolific hydrocarbon provinces (Dolson *et al.*, 2014). October oil field, one of the giant Gulf of Suez discoveries, 22 km², is located in the north-central part of the Gulf of Suez, 135 km SSW of Suez city (Kassem *et al.*, 2020). This study was applied on GS 305-2A Well.

The possible source rocks of Gulf of Suez have been examined by numerous authors. They suggested that the Lower Miocene Globigerina marls could be the possible source rocks of all the oil in the Gulf of Suez (Bobbitt and Gallagher, 1978). The most common Pre-Miocene oil sources, according to (Shahin and Shehab, 1984), are: Campanian brown limestone and Paleocene Esna shale, with sporadic periods of Matulla Formation. Furthermore, they proposed that oil in southern Gulf of Suez was originated from certain intervals of Lower Miocene age. Two significant sources of oil for hydrocarbons in the Red Sea and Gulf of Suez were categorized as unidentified according to Lindquist's clarification in the compiled report of US Geological Survey on the global energy project (Lindquist, 1998). The initial source comprises Campanian Sudr (Brown limestone/Dawi Formation) source rocks, whereas the second source involves the Middle Miocene Maqna source rocks.

The field produced oil from the pre-Miocene and Miocene clastic reservoir rocks including Lower Miocene Nukhul and Upper Rudeis Formations, Late Cretaceous formations and the Lower Cretaceous Nubia Sandstone (Radwan, 2021). Three opportunities in the October field can increase oil production and oil reserves for the field according to the most recent structural scenario work (Khattab *et al.*, 2023). In the southern part of the Gulf of Suez, the lower section of the Rudeis Formation is characterized by hydrocarbon generative potential. Thus, it can be classified as an active source rock (Elmaadawy *et al.*, 2021). From the previous decisions of (Radwan, 2021; Elmaadawy *et al.*, 2021), it can be concluded that Rudeis Formation can be considered as source and reservoir rock.

Formations that are widely considered as sources may be shales or lime-mudstones, which are rich in organic matter (TOC > 1 wt%). If the organic matter in good hydrocarbon source rocks attain a high enough degree of thermal maturity to produce and release commercial amounts of oil and/or

gas, the rock will produce hydrocarbons. Organic matter is present in non-source rocks; its amount is usually negligible (*Lindquist, 1998; Passey et al., 1990*).

Using a methodology based on density log and a combination of resistivity and porosity tools, this study seeks to estimate the total organic carbon content (TOC%) of the Rudeis Formation and analyze the portions of source rocks by calculating organic richness. Besides, the available output data of geochemical analyses from LECO and Rock-Eval pyrolysis 6 (TOC%, S1, S2, S3, Tmax) are utilized to evaluate the TOC content, organic richness, kerogen types, and thermal maturity. The potentialities of source rocks on basis of organic carbon richness can be classified as follows: poor source rock (TOC% < 0.5), fair source rock (TOC% 0.50–1.0), good source rock (TOC% 1.0–2.0) and very good source rock (TOC% > 2.0) (*Peters and Cassa, 1994*).

Depending on aerial spectral gamma-ray data survey in southwestern Sinai, the nearest area of Gulf of Suez, Rudeis Formation contains a very good hydrocarbon potentiality (*Shaheen et al., 2022*). In addition to using spectral gamma ray logs to determine hydrocarbon-bearing zones (Thorium normalization technique), Recently, it became possible to use statistical analysis of radiogenic heat generation derived from the amounts of radioactive materials in the rocks (K, eU, and eTh) to separate source rocks from reservoir rocks (*Nabih and Al-Alfy, 2021*).

The different petrophysical parameters of rocks as volume of shale, total & effective porosities, water & hydrocarbon saturations, etc..., can be calculated directly depending on conventional logs as gamma, neutron, density, resistivity and self-potential logs, using Techlog software (2015.3) and estimating the vertical litho-saturation cross-plot. All data used in this work were obtained under the license of the Egyptian Petroleum Corporation (EGPC).

2. Geological setting

October oil field, which is located between latitudes $28^{\circ} 46' 40''$ N and $28^{\circ} 57' 10''$ N and longitudes $32^{\circ} 57' 33''$ E and $33^{\circ} 10' 00''$ E is considered the oldest one in Gulf of Suez area (Fig. 1). More than 3000 metres of sediments ranging from Precambrian to Holocene were penetrated by several wells in this

oil field, as illustrated from the litho-stratigraphic section (Fig. 2) and modified by (Radwan *et al.*, 2020), where thick Miocene and Post-Miocene sediments are recorded as a series of parallel half grabens.

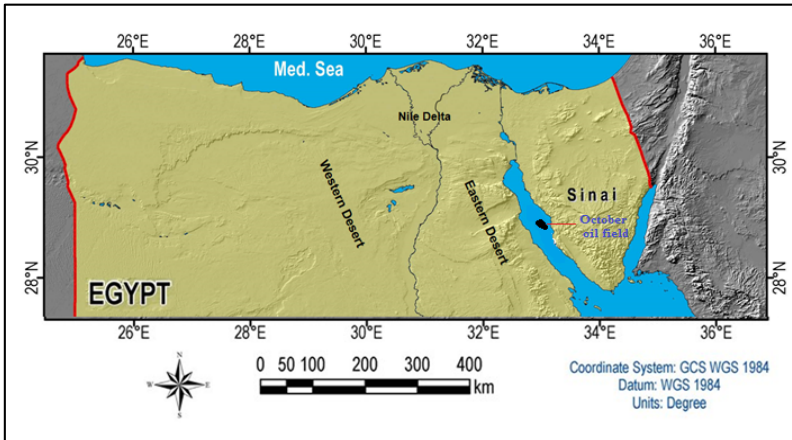


Fig. 1. Location map of October oil field, Gulf of Suez, Egypt.

Depending on the fact that the composition of lower Rudeis formation is marine shale and marls; Lower Rudeis formation is a source rock (Zahran, 1986; Wever, 2000). Meanwhile, the hydrocarbon produced from the sandstone of Upper Rudeis formation, (Khattab *et al.*, 2023).

Structurally, the pre-rift (pre-Miocene unit), syn-rift (Miocene unit) and post-rift (post-Miocene unit) sequences represent the three tectonic rift sequences, which divide Gulf of Suez according to the dip regime direction for each province (Darwish and El-Araby, 1993; EGPC, 1996; Bosworth and McClay, 2001). October oil field is dominated by four major fault trends and half grabens bounded by normal faults (Moustafa, 2004; Dolson *et al.*, 2014).

3. Methodology

Many different methodologies are used in this study, both theoretically and experimentally, to estimate the Radiogenic Heat Production (RHP) and total amount of organic carbon (TOC). Theoretically, porosity, resistivity, spectral gamma ray and density logs, among other well logging methods

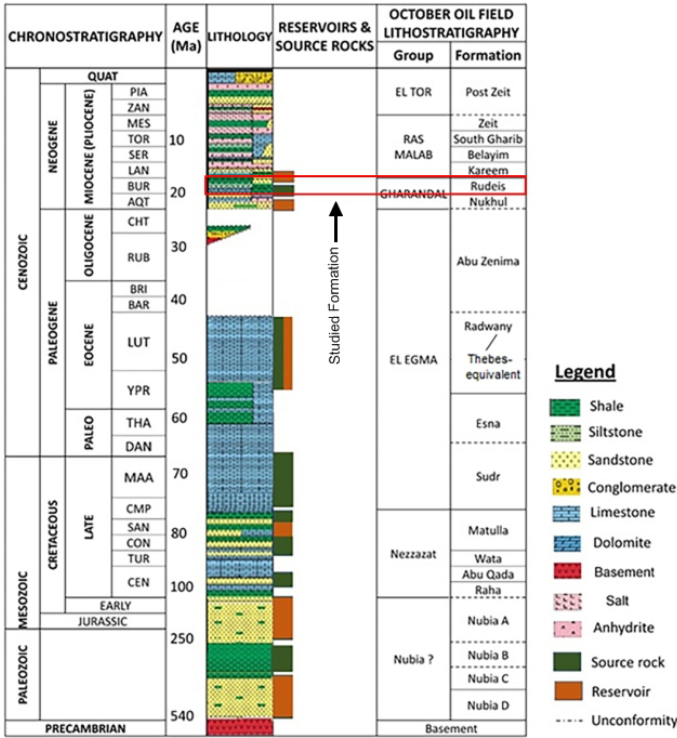


Fig. 2. Lithostratigraphic column of October oil field, Gulf of Suez, Egypt, modified after Shaheen et al. (2022).

were utilized. The TOC was computed using these tools in various techniques. Experimentally, the results of Rock-Eval pyrolysis as interpretative guidelines of source rock evaluation were used.

In the following sections, a detailed description of both methods is provided.

3.1. Total organic carbon from well logging

Many petrophysicists as Schmoker (1993); Passey et al. (1990); Klaja and Dudek (2016); Alshakhs and Rezaee (2017) over many years made attempts to calculate total carbon content values, based on conventional well logs as:

Schmoker (1993) equation:

$$TOC = (157/\rho_b) - 58.3, \tag{1}$$

Passey et al. (1990) equation:

$$\text{TOC} = \Delta \log R * 10^{[2.297 - (0.1688 * \text{LOM})]}, \quad (2)$$

Klaja and Dudek (2016) equation:

$$\text{TOC} = (0.1063 * U(\text{ppm})) - 0.009, \quad (3)$$

Alshakhs and Rezaee (2017) equation:

$$\text{TOC} = 8.24 + 0.0195 * \text{GR} + 0.12 * \text{Sonic} + 0.3 * \text{density}. \quad (4)$$

where, TOC is the total organic carbon, ρ_b is the bulk density, LOM is the level of metamorphism, U is the value of uranium, R represents the resistivity measurements (in Ohm.m), $\Delta \log R$ is the curve separation measured in logarithmic resistivity cycles, and Δt is the measured transit time (in sec/ft).

3.2. Radiogenic heat production (RHP)

The heat values resulting from the decay of radioactive isotopes present in rocks are called Radiogenic Heat Production (RHP) (*Hussain et al., 2024*). There are many uses for Radiogenic Heat Production property, which helps in analysing and evaluating the quality of hydrocarbon reservoirs. Recently, Radiogenic Heat Production was used to confirm the presence of hydrocarbons in the rocks and determine the association of these hydrocarbons with source or with reservoir rocks (*Nabih and Al-Alfy, 2021*).

An equation was derived by (*Rybach, 1986*) to calculate the RHP values, depending on the concentrations of the three radioactive elements (K, eU and eTh) and the densities of the rocks as:

$$\text{RHP} (\mu\text{W}/\text{m}^3) = 10^{-3} * \rho * [(95.2 * \text{eU}) + (25.6 * \text{eTh}) + (34.8 * \text{K})]. \quad (5)$$

Because gamma ray logs are recorded in all hydrocarbon wells, while spectral gamma ray logs are less recorded, scientists (*Bücker and Rybach, 1996*) derived an equation to calculate RHP values from total gamma ray log as:

$$\text{RHP} (\mu\text{W}/\text{m}^3) = 0.0158 [\text{GR}(\text{api}) - 0.8]. \quad (6)$$

3.3. Reservoir parameters

The hydrocarbon potentiality of the two studied members is investigated through conducting complete logging analyses. The different formation eval-

uation parameters are estimated using the quantitative procedures. The most important parameters of these parameters are those of volume of shale, fluid saturation, hydrocarbon saturation, total and effective porosity and lithology type, shallow and deep resistivity, using Techlog software. Gamma ray log is used mainly for shale volume determination, while neutron and density logs are used to derive porosity. The resistivity ratio is used to estimate the apparent water resistivity and the widely known simultaneous equations are applied for lithology determination. Uranium isn't a component of clay minerals, thus, to avoid its radiation effect, a computed gamma-ray (CGR) log was used to calculate the accurate volume of shale percentage in different rocks (*Nabih and Al-Alfy, 2018*).

3.4. TOC from geochemical measurements

The quantity of organic matter in the source rock determines its hydrocarbons generation potential (*Tissot and Welte, 1984*).

Laboratory measurements for calculating total organic content values are accurate and reliable. However, it requires cost and time to perform these measurements.

In the present work, Rock Eval Pyrolysis method was applied and the analyses were carried out in the Egyptian Petroleum Research Institute (EPRI) using Rock-Eval 6 analyser. The evaluation of source rocks is based on the pyrolysis analysis data, such as: Total Organic Carbon (TOC), Hydrocarbon Potentiality (S2), Production Index (PI), Oxygen Index (OI), Hydrogen index (HI) and maximum temperature (Tmax). The Rock Eval pyrolysis data of the studied samples are given on Table 1. Organic richness, genetic types of organic matter and thermal maturation of these samples are discussed in the following item.

4. Results and discussions

The combined litho-saturation cross plot of the GS 305-2A Well is shown on Fig 3. Rudeis Formation is extended between depths of 7660 to 10460 ft. The upper section of Upper Rudeis was between 7660 and 8409 feet, while the lower part was between 8409 and 10460 feet. The upper Rudeis is composed of shale with little sandstone interbedded through it, but the lower Rudeis members are primarily composed of sandstone and shale. Both the

Table 1. Rock Eval Pyrolysis data of the studied samples, Rudeis Formation, Gulf of Suez, Egypt.

Well Name	Formation Name	Depth (ft)	TOC (wt%)	S2 (mg/g)	TMAX (degC)	(HI)	(OI)	(PI)
GS 305-2A Well	Upper Rudeis	7650	0.48	0.74	427	156	301	0.15
		7700	0.65	0.83	430	128	309	0.12
		7750	0.54	0.58	433	107	172	0.17
		7800	0.42	0.49	426	117	243	0.2
		7850	0.44	0.46	428	105	189	0.19
		7950	0.5	0.98	428	196	498	0.24
		8000	0.57	0.97	430	170	246	0.18
		8050	0.75	0.88	432	117	145	0.17
		8100	0.59	0.96	434	163	302	0.18
		8150	0.93	1.96	431	211	131	0.12
		8250	0.62	1.37	432	221	331	0.17
		8300	1	2.37	434	237	166	0.12
		8400	0.68	0.99	433	146	193	0.16
		8450	0.67	1.17	433	175	321	0.16
		8500	0.76	1.37	432	180	228	0.14
		8550	0.94	2.38	434	253	202	0.11
		8600	0.97	2.31	432	238	220	0.13
		8650	0.8	2.05	431	256	275	0.15
		8700	0.71	1.4	432	197	377	0.15
		8750	0.71	1.2	433	169	370	0.15
		8800	0.98	2.36	434	241	221	0.12
		8850	0.9	2.3	437	256	324	0.14
		8900	1.1	3.12	432	284	280	0.13
		8950	1.14	2.92	437	256	268	0.11
		9000	0.77	1.37	437	178	288	0.1
		9050	1.08	2.98	436	276	329	0.14
		9100	1.29	3.57	436	277	205	0.11
		9150	0.89	2.34	436	263	236	0.11
9200	0.76	1.79	436	236	268	0.13		
9250	0.81	1.55	437	191	383	0.13		
9300	0.98	2.21	435	226	217	0.11		
9350	0.89	1.88	436	211	381	0.15		

Table 1. Continued from the previous page.

Well Name	Formation Name	Depth (ft)	TOC (wt%)	S2 (mg/g)	TMAX (degC)	(HI)	(OI)	(PI)
GS 305-2A Well	Lower Rudeis	9400	0.73	1.76	438	241	362	0.15
		9450	0.74	1.88	437	254	253	0.14
		9500	1.02	2.17	436	213	255	0.15
		9550	0.87	1.35	437	155	244	0.13
		9600	1.28	3.76	435	294	205	0.14
		9650	0.72	1.75	434	243	275	0.14
		9700	0.47	0.88	438	187	257	0.15
		9750	0.73	1.75	438	240	237	0.15
		9850	0.79	0.94	432	119	156	0.15
		9900	0.92	2.17	433	236	235	0.14
		9950	0.95	2.55	436	268	214	0.13
		10000	0.79	2.14	436	271	304	0.14
		10050	0.97	1.53	439	158	193	0.14
		10300	1.04	1.88	436	181	210	0.15
		10350	0.87	1.94	433	223	138	0.14
10400	0.46	2.48	437	539	180	0.12		
10450	0.91	1.45	436	159	76	0.11		

upper and lower Rudeis members have high values of shale content. Values of 63% and 51% are recorded for Upper and Lower members respectively, and both have hydrocarbon saturation rates of 57% to 60%. On the other side of the shale lithology, the water saturation (last track) curve displays a low value that was derived from archie/s Equation. It is recorded 54 and 40.5 for Upper and Lower Rudeis, respectively.

The presence of clay minerals is shown by a thorium-potassium crossplot (Halliburton, 1995), which directly affects reservoir and source efficiency. A distinct cluster can be seen on Fig. 4a in the montmorillonite and mixed layer sections, together with small amounts of mica, illite, and chlorite. But, when the (Th/K and Th/U ratios) crossplot (Fig. 4b) is used, the mixed layer (illite–montmorillonite) appears to be the predominant clay type.

The calculated Radiogenic Heat Production (RHP) values related to Rudeis formation deposits were analysed statistically (Eq. (6)). They range from $0.85 \mu\text{W}/\text{m}^3$ as a minimum value to $2.38 \mu\text{W}/\text{m}^3$ as a maximum value,

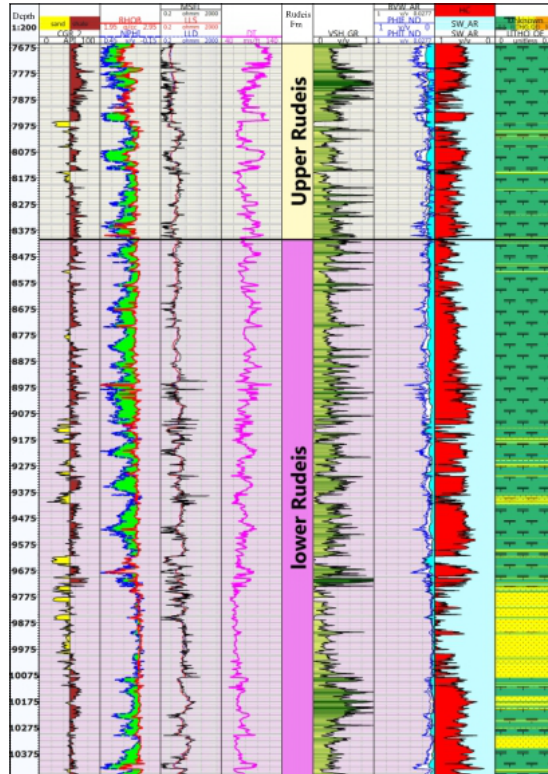


Fig. 3. Combined litho-saturation cross plot of Rudeis Formation in GS 305-2A Well, October oil field, Gulf of Suez, Egypt.

while $1.37 \mu\text{W}/\text{m}^3$ values represents the mean RHP value, with a standard deviation (St.D.) value of $0.19 \mu\text{W}/\text{m}^3$. Figure 5 illustrates the radiogenic heat output in the final track, which ranges from 0 to $2.5 \mu\text{W}/\text{m}^3$. The mean RHP value along the Upper and Lower Rudeis formations in the study well is indicated by the first red line in the RHP zone, and the mean (RHP + 1 St.D.) value, is indicated by the second black line. Zones without hydrocarbon materials are represented by values less than $0.81 \mu\text{W}/\text{m}^3$, which include those between 7840 feet and 7950 feet, 9040 feet and 9130 feet, and 9780 feet and 9920 feet. Zones that are saturated by hydrocarbon compounds and have values more than $0.81 \mu\text{W}/\text{m}^3$ can be divided into two categories. The values in the first category, which range from $0.81 \mu\text{W}/\text{m}^3$ to $1.36 \mu\text{W}/\text{m}^3$, are associated with zones that correspond with rocks in the

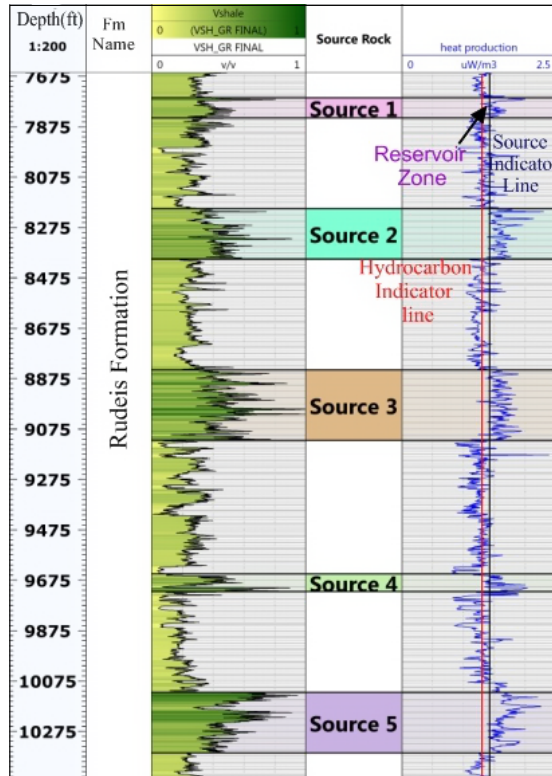


Fig. 5. Vertical distribution of Radiogenic Heat Production (RHP) and Volume of shale (Vsh) values of Rudeis Formation, in GS 305-2A Well, October oil field, Gulf of Suez, Egypt.

Rudeis member is classified as a fair oil source rock, based on TOC values that are shown before, and Hydrogen Index (HI) values that range from 105–284 mg HC/g. Lower Rudeis formation is classified as a fair to good oil source rock based on TOC values and 119–547 mg HC/g for HI values (Fig. 8). Nearly all of the study samples are over the production index line (0.1), which indicates a considerable degree of conversion, according to PI vs. Tmax (Fig. 9).

Figure 10 shows the relationship between laboratory and calculated TOC values. As seen in the same figure, lots of equations were used such as Eqs. (1), (2) and (3), and (4). Not all of them match with the laboratory data such as Eq. (4) where its results were illogically (*Alshakhs and Rezaee,*

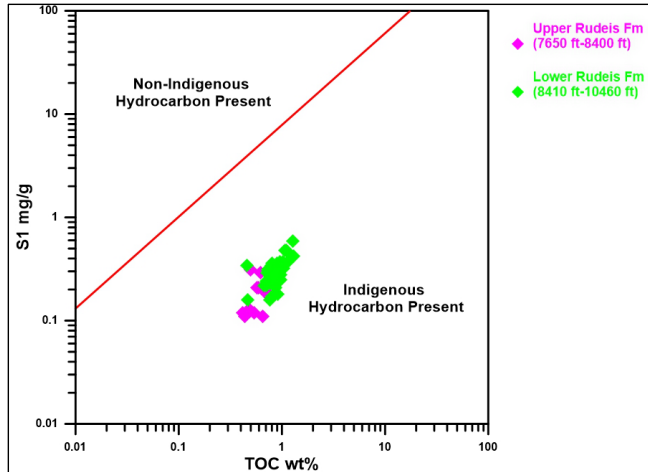


Fig. 6. Diagram of S1 against TOC adapted from (Jarvie et al., 2001). Rudeis Formation, in GS 305-2A Well, October oil field, Gulf of Suez, Egypt.

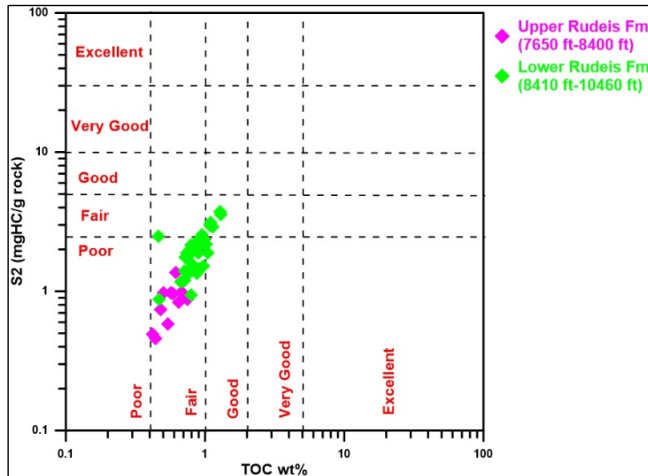


Fig. 7. Diagram of S2 versus TOC adapted from (Peters and Cassa, 1994). Rudeis Formation, in GS 305-2A Well, October oil field, Gulf of Suez, Egypt.

2017). The promised Eqs. (1), (2) and (3) matched with the geochemical results. These results are completely logically matched with Eqs. (1), (2) and (3). Meanwhile, the results of applying these equations were relatively consistent with laboratory values. The laboratory measurements of TOC

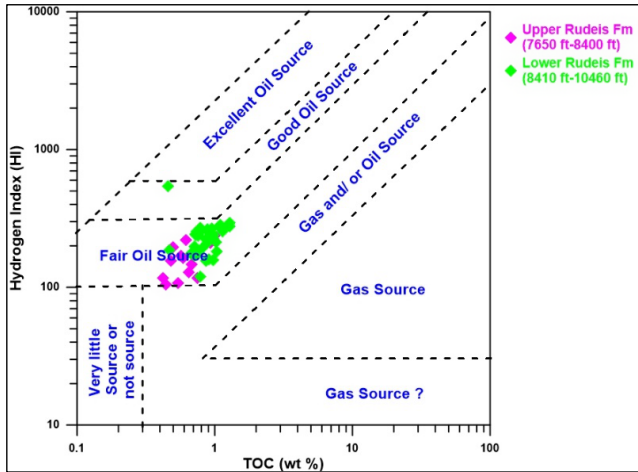


Fig. 8. Diagram of HI against TOC adapted from (Delvaux et al., 1990). Rudeis Formation, in GS 305-2A Well, October oil field, Gulf of Suez, Egypt.

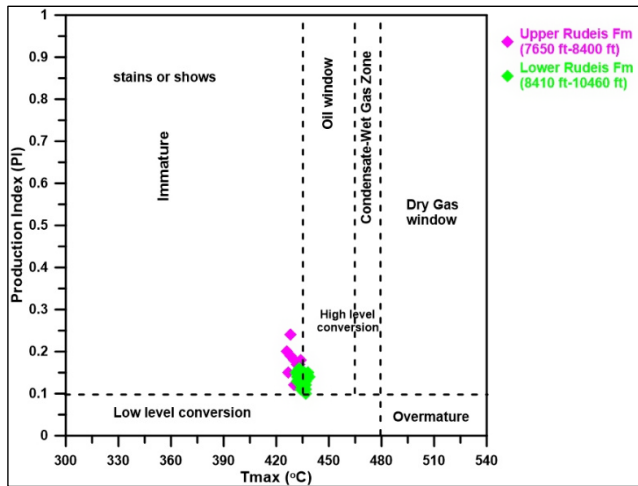


Fig. 9. Cross plot of PI against Tmax diagram adapted from (Delgado et al., 2018). Rudeis Formation, in GS 305-2A Well, October oil field, Gulf of Suez, Egypt.

values in the study rock samples range from 0.4% to 1.4% with mean value of 0.9%. On the other hand the mean TOC value calculated theoretically from Eqs. (1), (2) and (3) is 1.2%. Therefore, the results of these equations can be adopted to calculate TOC values, and these confirm the theory of

optimum conditions for application, which acknowledges that a single theory cannot be applied in different cases, but rather that each case has its own theory to be applied. Equations (1), (2) and (3) were the most accurate in matching the TOC results.

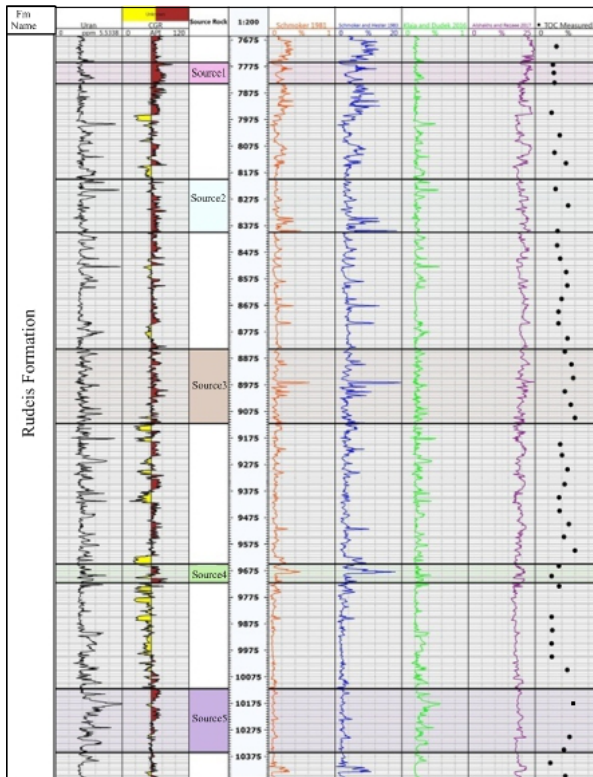


Fig. 10. Relationship between laboratory and theoretical calculations of TOC values in GS 305-2A Well, Rudeis Formation, October oil field, Gulf of Suez, Egypt.

5. Conclusions

The predominant lithologies found in the studied well are sandstone and shale. Using the spectral gamma-ray logs, several crossplots were made in order to get the best interpretation of reservoir and source zones, the predominated clay types in the study well were montmorillonite, mixed layer, illite, and chlorite in upper and lower Rudeis formation.

Both the upper and lower Rudeis formations have shale content percentages of 63% and 51%, respectively, and both have hydrocarbon saturation rates of 57% to 60%.

The Radiogenic Heat Production values of Rudeis formation range from $0.85 \mu\text{W}/\text{m}^3$ as a minimum value to $2.38 \mu\text{W}/\text{m}^3$ as a maximum value, and $1.37 \mu\text{W}/\text{m}^3$ as a mean calculated RHP value, with a standard deviation value of $0.19 \mu\text{W}/\text{m}^3$. Five sections along Rudeis Formation named Source 1 to Source 5 (Fig. 5) considered hydrocarbon-bearing zones. three of them classified as source rock (Source 2, Source 3, and Source 5) that linked to the high volume of shale values (mostly clay), while the other two zones (Source 1 and Source 4) were linked to the moderate volume of shale values (shaly sandstone) zones, considered as source and reservoir rocks in Upper and Lower Rudeis formation.

All of the geochemical samples are over the production index line (0.1), which indicates a considerable degree of conversion, according to the Production Index (PI) vs. maximum temperature (Tmax). Lower Rudeis member is evaluated as having fair to good hydrocarbon potential source rock, with TOC ranging from 0.46 to 1.28 weight percent and S2 varying from 0.88 to 3.76 mg/g, while upper Rudeis member is classified as a fair oil source rock, based on TOC values ranging from 0.42 to 1.29 weight percent.

Laboratory measurements of TOC values in the studied rock samples agree well with the values which are calculated theoretically using Eqs. (1), (2) and (3). Therefore, the results of these equations can be adopted to calculate TOC values.

References

- Alshakhs M., Rezaee R., 2017: A new method to estimate total organic carbon (TOC) content; an example from Goldwyer shale formation, Canning Basin. *Open Petrol. Eng. J.* **10**, 118–133, doi: 10.2174/1874834101710010118.
- Bobbit J. E., Gallagher J. O., 1978: The Petroleum Geology of the Gulf of Suez. In: 10th Annual Offshore Technical Conference, Houston, 8-10 May 1978, OTC-3091-MS, pp. 375–380, doi: 10.4043/3091-MS.
- Bosworth W., McClay K., 2001: Structural and stratigraphic evolution of the Gulf of Suez rift, Egypt: A synthesis. In: Ziegler P. A., Cavazza W., Robertson A. H. F., Crasquin-Soleau S. (Eds.): Peri-Tethys Memoir 6: Peri-Tethyan Rift/Wrench Basins and Passive Margins. *Mem. Mus. Natl. Hist. Nat.*, **186**, pp. 567–606.
- Bücker C., Rybach L., 1996: A simple method to determine heat production from gamma-ray logs. *Mar. Pet. Geol.*, **13**, 4, 373–375, doi: 10.1016/0264-8172(95)00089-5.

- Darwish M., El-Araby A. M., 1993: Petrography and diagenetic aspects of some siliciclastic hydrocarbon reservoirs in relation to rifting of Gulf of Suez. In: Philobos E. R., Purser B. H. (Eds.): *Geodynamics and Sedimentation of the Red Sea–Gulf of Aden Rift System*. Geol. Soc. Egypt, Spec. Publ., 1, pp. 155–187.
- Delgado L., Batezelli A., Luna J., 2018: Petroleum geochemical characterization of Albian-Oligocene sequences in the Campos Basin: “Case study: Eastern Marlim oil field, offshore, Brazil”. *J. S. Am. Earth Sci.*, **88**, 715–735, doi: 10.1016/j.jsames.2018.10.009.
- Delvaux D., Martin H., Leplat P., Paulet J. 1990: Geochemical characterization of sedimentary organic matter by means of pyrolysis kinetic parameters. *Org. Geochem.*, **16**, 1–3, 175–187, doi: 10.1016/0146-6380(90)90038-2.
- Dolson J. C., Atta M., Blanchard D., Sehim A., Villinski J., Loutit T., Romine K., 2014: Egypt’s future petroleum resources: A revised look in the 21st century (Chapter 5). In: Marlow L., Kendall C. C. G., Yose L. A. (Eds.): *Petroleum Systems of the Tethyan Region*, **106**, AAPG Mem., pp. 143–178., doi: 10.1306/13431856M106713.
- EGPC, Egyptian General Petroleum Corporation, 1996: *Gulf of Suez oil fields (A comprehensive overview)*. EGPC, Cairo, 736 p.
- Elmaadawy K. G., Elbassiouny H. A. M., Raslan S. M., 2021: Thermal maturity and hydrocarbon generation modelling for the Lower Rudeis source rock and petroleum system analysis in Garra area, South Gulf of Suez, Egypt. *J. Pet. Min. Eng.*, **23**, 1, 65–81, doi: 10.21608/jpme.2021.62686.1071.
- Halliburton, 1995: Interpretation of the spectral gamma log. Haliburton Ledger.
- Hussain W., Luo M., Ali M., Al-Khafaji H. F., Hussain I., Hussain M., Ahmed S. A. A., Obaidullah, 2024: A Gamma-ray spectroscopy approach to evaluate clay mineral composition and depositional environment: A case study from the lower Goru Formation, Southern Indus Basin, Pakistan. *J. Appl. Geophys.*, **226**, 105414, doi: 10.1016/j.jappgeo.2024.105414.
- Jarvie D. M., Morelos A., Han Z., 2001: Detection of pay zones and pay quality, Gulf of Mexico: Application of geochemical techniques. *GCAGS Trans.*, **51**, 151–160.
- Kassem A. A., Sharaf L. M., Baghdady A. R., El-Naby A. A., 2020: Cenomanian/Turonian oceanic anoxic event 2 in October oil field, Central Gulf of Suez, Egypt. *J. Afr. Earth Sci.*, **165**, 103817, doi: 10.1016/j.jafrearsci.2020.103817.
- Khattab M. A., Radwan A. E., El-Anbaawy M. I., Mansour M. H., El-Tehiwy A. A., 2023: Three-dimensional structural modelling of structurally complex hydrocarbon reservoir in October Oil Field, Gulf of Suez, Egypt. *Geol. J.*, **58**, 11, 4146–4164, doi: 10.1002/gj.4748.
- Klaja J., Dudek L., 2016: Geological interpretation of spectral gamma ray (SGR) Logging in selected boreholes. *Nafta-Gaz*, **72**, 1, 3–14, doi: 10.18668/NG2016.01.01.
- Lindquist J. S., 1998: *The Red Sea Basin Province: Sudr-Nubia and Maqna Petroleum Systems*. U.S. Department of the Interior, U.S. Geological Survey, Open File Report No. 99-50-A, 21 p.
- Moustafa A. R., 2004: Exploratory notes for the geologic maps of the eastern side of the Suez rift (western Sinai Peninsula), Egypt. AAPG Bull., Datapages, Inc. GIS Series, 34 p.

- Nabih M., Al-Alfy I. M., 2018: New approach for releasing uranium radiation impact on shale content evaluation in shaly sand Formations: A case study, Egypt. *Appl. Radiat. Isot.*, **141**, 33–43, doi: 10.1016/j.apradiso.2018.08.002.
- Nabih M., Al-Alfy I. M., 2021: Differentiation between source and reservoir rocks using statistical analysis of radiogenic heat production: A case study on Alam El Bueib Formation, North Western Desert, Egypt. *Appl. Radiat. Isot.*, **176**, 109868, doi: 10.1016/j.apradiso.2021.109868.
- Passey Q. R., Creaney S., Kulla J. B., Moretti F. J., Stroud J. D., 1990: A practical model for organic richness from porosity and resistivity logs. *AAPG Bull.*, **74**, 12, 1777–1794, doi: 10.1306/OC9B25C9-1710-11D7-8645000102C1865D.
- Peters K. E., Cassa M. R., 1994: Applied source rock geochemistry (Chapter 5). In: Magoon L. B., Dow W. G. (Eds.): *The petroleum system—from source to trap*. AAPG Mem., **60**, Tulsa, 93–120, doi: 10.1306/M60585C5.
- Radwan A. E., 2021: Modeling the depositional environment of the sandstone reservoir in the middle Miocene Sidri Member, Badri field, Gulf of Suez Basin, Egypt: Integration of gamma-ray log patterns and petrographic characteristics of lithology. *Nat. Resour. Res.*, **30**, 1, 431–449, doi: 10.1007/s11053-020-09757-6.
- Radwan A. E., Abudeif A. M., Attia M. M., Elkhawaga M. A., Abdelghany W. K., Kasem A. A., 2020: Geopressure evaluation using integrated basin modelling, well-logging and reservoir data analysis in the northern part of the Badri oil field, Gulf of Suez, Egypt. *J. Afr. Earth Sci.*, **162**, 103743, doi: 10.1016/j.jafrearsci.2019.103743.
- Rybach L., 1986: Amount and significance of radioactive heat sources in sediments. In: Burrus J. (Ed.): *Thermal Modelling in Sedimentary Basins*. Collection Colloquies Seminars, **44**, Éditions Technip, Paris, pp. 311–322.
- Schmoker J., 1993: Use of formation-density logs to determine organic-carbon content in Devonian shales of Western Appalachian basin and an additional example based on the Bakken formation of Williston Basin (Chapter J). In: Roen J. B., Kepferle R. C. (Eds.): *Petroleum Geology of the Black Shale of Eastern North America*. U.S. Geol. Surv. Bull., 1909, p. J1–J14.
- Shaheen M. A., Abd El Salam H. F., El Hawary A. M., 2022: Aerial gamma-ray spectrometric data as a guide for probable hydrocarbon accumulations at Abu-Zeneima/Al-Tur area, Southwestern Sinai, Egypt. *Appl. Radiat. Isot.*, **186**, 110290, doi: 10.1016/j.apradiso.2022.110290.
- Shahin A. N., Shehab M. M., 1984: Petroleum generation, migration and accumulation in the Gulf of Suez offshore, Sinai. In: 6th E.G.P.C, Exploration Seminar, Vol. 1, pp. 126–152.
- Tissot B. P., Welte D. H., 1984: Kerogen: composition and classification. In: *Petroleum Formation and Occurrence*. Springer, Berlin, Heidelberg, pp. 131–159, doi: 10.1007/978-3-642-87813-8_9.
- Wever H. E., 2000: Petroleum and source rock characterization based on C₇ star plot results: Examples from Egypt. *AAPG Bull.*, **84**, 7, 1041–1054, doi: 10.1306/A9673BA8-1738-11D7-8645000102C1865D.
- Zahran M. E., 1986: Geology of October oilfield. In: *Proc. EGPC 8th Expl. Conf.*, Cairo, Egypt, pp. 52–53.